agronomy

MDPI

Article

Genomic Regions Influencing Preharvest Sprouting Tolerance in Two Doubled-Haploid Wheat Populations (*Triticum aestivum* L.)

Thobeka Phililе Khumalo [1,2,*], Tsepiso Hlongoane [1], Annelie Barnard [1] and Toi John Tsilo [1,2]

[1] Germplasm Department, Agricultural Research Council–Small Grain, Bethlehem 9700, South Africa; hlongoanet@arc.agric.za (T.H.); abarnard2812@gmail.com (A.B.); tsilot@arc.agric.za (T.J.T.)
[2] Department of Life and Consumer Sciences, University of South Africa, Florida 1710, South Africa
* Correspondence: thobekaphilile@outlook.com

Abstract: The current and projected climate change that is represented by increasing temperatures and humidity levels and irregular rainfall patterns promotes the occurrence of preharvest sprouting (PHS) in wheat. PHS results in significant economic losses, globally, which necessitates the need for high-yielding cultivars with increased PHS tolerance; hence, this study was conducted. The current study evaluated two doubled-haploid (DH) wheat populations of Tugela-Dn × Elands and Elands × Flamink across six environments in the Free State Province of South Africa to select genotypes with increased PHS tolerance and further map the underlying loci. Significant effects of DH lines (194) and environments (6) were observed for PHS tolerance. The results of this study validate previous findings that PHS is only expressed when environmental conditions are conducive. Quantitative trait loci (QTL) mapping using single-nucleotide polymorphism (SNP) and silicoDArT markers revealed three additive QTLs with major effects on chromosomes 5B and 7B, and these QTLs were detected more than once, when conditions were favourable. These QTLs explained a phenotypic variation (PVE) varying between 10.08% and 20.30% (LOD = 2.73–3.11). About 16.50% of DH lines performed to the level of Elands (the PHS-tolerant parent) and are recommended for further selection in a pre-breeding or breeding programme. The findings of this study are expected to expedite the on-going breeding efforts for PHS tolerance in winter wheat, which will facilitate the development of PHS-tolerant cultivars adapted to the South African environment.

Keywords: phenotypic selection; preharvest sprouting tolerance; QTL mapping analysis; silicoDArT; SNP; wheat

Citation: Khumalo, T.P.; Hlongoane, T.; Barnard, A.; Tsilo, T.J. Genomic Regions Influencing Preharvest Sprouting Tolerance in Two Doubled-Haploid Wheat Populations (*Triticum aestivum* L.). *Agronomy* **2022**, *12*, 832. https://doi.org/10.3390/agronomy12040832

Academic Editor: Jian Ma

Received: 25 January 2022
Accepted: 3 March 2022
Published: 29 March 2022

1. Introduction

Preharvest sprouting (PHS) is the premature germination of kernels on physiologically mature wheat ears upon continuous wet and humid conditions during the harvest season [1,2]. This phenomenon has resulted in a significant reduction in wheat grain yield and end-use quality, worldwide [3–6]. This is due to the activation of enzymes such as lipases, amylases and proteases in developing kernels, which leads to the degradation of lipids, starch and proteins [7,8] and thus reduces the market value of wheat grain by up to 50% [4,9,10]. Annual grain yield and end-use quality losses due to PHS are estimated above USD 1 billion, worldwide [5,11,12].

PHS tolerance remains a trait of interest in the South African (SA) wheat production, especially amid the current and forecasted climatic change that significantly impacts grain yield and quality [13,14]. Most of the wheat production regions in the country receive summer rainfall around harvest, which puts the production at high risk of PHS [15–19]. Various methods have been used to evaluate and improve PHS tolerance in released commercial cultivars [20]. A visual screening test of more than 2% sprouted kernels per 25 g wheat sample together with a falling number below 220 s has been used to downgrade

wheat to lower grades, such as grades B1 to B3, depending on the protein content and hectolitre mass [20–22].

Significant improvement in PHS tolerance in bread wheat, especially winter cultivars, has been achieved in SA over the years through conventional breeding [23]. Most current commercial cultivars either have good or moderate PHS tolerance [20]. This improvement has resulted in extensive genetic diversity in PHS tolerance [21,23,24], which has been used in wheat breeding programmes across the country. The use of molecular markers in breeding for PHS tolerance and to identify lines with potential tolerance to PHS has only been incorporated recently in wheat breeding programmes in the country [25].

The identification of genomic regions and associated molecular markers influencing PHS tolerance is anticipated to speed up the development of PHS-tolerant cultivars that are adapted to the SA environment. However, the complex nature of PHS tolerance and the interaction between associated genes and the environment can cause the cultivars' level of tolerance to PHS to vary from year to year [25–27]. This makes selection for high-yielding varieties with increased PHS tolerance, which are stable across environments and years, challenging, especially under the current and predicted climate change6 [28].

Contrastingly, more progress has been attained in breeding for PHS tolerance (alongside other grain yield-related traits) through MAS in most parts of the world [6,29–40]. These studies proved an extensive genotypic variation for PHS tolerance as a result of the complex genetic nature of this trait. This variation has been further utilised in wheat breeding programmes and exchanged globally. Moreover, negative correlations between PHS tolerance and grain yield, seed viability, seedling vigor, flour yield and baking quality have been reported [10,27,41,42], proving the importance of this trait in the improvement in grain yield and quality. Therefore, understanding the genetics of PHS tolerance in wheat can accelerate the needed improvements in grain yield and quality [43–47]; nonetheless, plant adaptation remains vital in the overall plant performance [48].

The present study was conducted to evaluate PHS tolerance in bread wheat winter lines planted across multiple environments to select doubled-haploid (DH) lines with increased PHS tolerance and further map the underlying loci. The study objectives were to (1) examine the performance of DH lines and parents with regard to PHS tolerance across six environments; (2) identify quantitative trait loci (QTLs) controlling PHS tolerance in the Tugela-Dn × Elands DH population; and (3) validate the presence of detected QTLs in a population with a different genetic background, Elands × Flamink.

2. Materials and Methods

2.1. Plant Material, Study Area and Experimental Design

Two DH wheat populations ($n = 210$) derived from two crosses of Tugela-Dn × Elands [49] and Elands × Flamink [50] and the three respective parents as checks (Tugela-Dn, Elands and Flamink) were provided by the Agricultural Research Council–Small Grain Germplasm Bank and evaluated for PHS tolerance. The Tugela-Dn × Elands DH population [49] was specifically developed to evaluate PHS tolerance and grain yield-related traits attributed to the two widely used parents with contrasting reactions to PHS, adaptability and grain morphological characteristics [51,52]. Tugela-Dn is a winter wheat cultivar highly susceptible to PHS; however, it has a high yield potential. This cultivar has been extensively used for dryland wheat production in South Africa, since 1992. Elands is a facultative cultivar that was released for dryland wheat production in 1998. This cultivar has a high yield potential, excellent tolerance to PHS and exceptional bread-making quality, which makes it a quality standard in the South African wheat industry [50]. The Flamink parental cultivar of the Elands × Flamink DH population [50] has vernalisation requirements and a high yield potential; however, it exhibits a reduced level of tolerance to PHS.

This study was conducted in six environments in the Free State Province of South Africa over two years, 2016 and 2017. Environments included Arlington 2016 (ARL1), Bethlehem 2016 (BHM3), Bethlehem 2017 (BHM4), Clarens 2016 (CLAR5), Harrismith 2016 (HAR7) and Harrismith 2017 (HAR8). The respective locations and weather descriptions

of the six environments are shown in Table 1. An augmented design was used in all environments as described in Khumalo et al. [50]. A single replicate of each DH line and five replicates of the three parents were grown in 1 m rows with an inter-row and intra-row spacing of 0.45 and 0.5 m, respectively. Commercial production and agronomic practices were followed as recommended for the specific production region.

Table 1. Descriptions of the six study environments between grain filling, maturity and harvest stages of wheat in 2016 and 2017 planting seasons. The weather data for the six environments are only shown for the months when the wheat plant was still in the field, from the grain filling stage until harvest.

† Env	Period	‡ Geographic Position			*Average Daily Temperature (°C)*		*Average Daily Humidity (%)*		*Average Daily Rainfall (mm)*
		Longit.	**Latit.**	**Altit. ‡ (m.a.s.l.)**	**Min**	**Max**	**Min**	**Max**	
ARL1	October 2016	26.7732	28.0046	1435	12.67	27.00	28.33	48.67	1.66
	November 2016				17.67	31.33	33.00	62.67	0.02
	December 2016				18.67	31.67	30.00	52.00	0.03
	January 2017				17.33	31.33	26.00	46.00	0.00
BHM3	October 2016	28.2973	−28.1628	1721	11.00	26.00	33.50	92.50	1.38
	November 2016				14.05	27.26	35.25	94.40	4.01
	December 2016				13.63	27.94	37.29	93.77	3.11
	January 2017				13.32	26.20	41.65	94.53	4.56
BHM4	October 2017	28.2973	−28.1628	1721	7.06	24.61	27.28	90.13	1.39
	November 2017				9.04	26.76	25.27	90.81	3.14
	December 2017				12.23	26.66	35.84	93.01	3.69
CLAR5	October 2016	28.5838	−28.5038	1849	8.17	25.47	18.71	84.18	1.22
	November 2016				11.37	25.38	34.19	92.64	3.45
	December 2016				12.36	27.24	33.54	92.50	3.73
	January 2017				12.30	25.00	41.07	93.13	3.90
HAR7	October 2016	29.11596	−28.3128	1720	9.17	25.85	23.08	87.88	1.42
	November 2016				12.09	25.42	42.99	91.43	4.43
	December 2016				13.18	27.45	42.06	89.57	4.60
	January 2017				12.66	26.58	47.29	89.68	5.54
HAR8	October 2017	29.11596	−28.3128	1720	7.65	24.89	30.41	84.01	1.6
	November 2017				9.76	27.05	28.93	80.81	2.73
	December 2017				11.93	26.05	42.76	89.45	6.74

† Environment denotes ARL1 for Arlington 2016, BHM3 for Bethlehem 2016, BHM4 for Bethlehem 2017, CLAR5 for Clarens 2016, HAR7 for Harrismith 2016 and HAR8 for Harrismith 2017. In BHM4 and HAR8, wheat was harvested in December 2017; therefore, no weather data are shown for January 2018. ‡ Geographic position denotes Longit. for longitude, Latit. for latitude and Altit. for altitude. ‡ m.a.s.l. denotes metres above sea level.

2.2. Phenotypic Evaluation of PHS Tolerance

At the anthesis stage, 28 ears per DH line and parent were randomly tagged using insulation tape. As described by Barnard et al. [15], the tagged wheat ears were hand-harvested at physiological maturity, air-dried at room temperature and stored in a cold room (4 °C) to maintain dormancy until PHS evaluation. Wheat ears were then subjected to simulated rainfall in a humidified chamber at 15 °C/25 °C day/night temperature with 98% humidity for 72 h and eventually scored for PHS tolerance according to a rating scale of 1 (not sprouted)–8 (highly sprouted) (Figure S1; [15]).

2.3. Phenotypic Evaluation and Statistical Analysis

Statistical analyses were performed in Genstat 18th Edition [53] using 194 DH lines (139 Tugela-Dn × Elands + 55 Elands × Flamink) following the removal of DH lines with missing data in most of the environments. Data were tested for normality using the Shapiro–Wilk test and the Wilcoxon matched-pairs test prior to conducting the analysis of variance (ANOVA). ANOVA and the non-parametric Kruskal–Wallis test were used to examine significant effects of genotypes, environments and the genotype × environment interaction. The genotype × environment interaction was estimated from the error mean square (MS_{ge}) of the replicated parents within environments according to an augmented design defined by Federer [54]. Patterns of genotype × environment interaction and genotype stability

were illustrated on the additive main effects and multiplicative interaction (AMMI) biplot, and the frequency distribution of phenotypes in the six environments was depicted in histograms. The broad-sense heritability (H^2) estimate of PHS tolerance was calculated using the following formula [55]:

$$1 - \frac{MSge}{MSg} \text{ or } \frac{\sigma^2 g}{[\sigma^2 g + \left(\frac{\sigma^2 ge}{e}\right) + \left(\frac{\sigma^2 \mathrm{e}}{re}\right)]}$$

where MS_{ge} and MS_g represent the genotype × environment and the genotype mean squares, respectively; $\sigma^2 g$ is the genotypic variance = $(\frac{MSg - MSge}{re})$; $\sigma^2 ge$ is the genotype × environment interaction variance = $\frac{MSge - MSe}{r}$; e and r represent the number of environments and replications, respectively; and $\sigma^2 e$ is the error variance = MS_e.

2.4. Genotyping and Construction of Genetic Map

The total genomic DNA was extracted from fresh leaves of three-week-old plants of 194 DH lines and 3 parents according to the Diversity Arrays Technology (DArT) plant DNA extraction protocol (https://www.diversityarrays.com/orderinstructions/plant-dna-extraction-protocol-for-dart/; accessed on 20 March 2019). The extracted DNA was genotyped with the DArT-sequencing genotype-by-sequence (GBS) platform 1.0 (DArT, Pty Ltd., Yarralumla, ACT, Australia), which produced 3204 single-nucleotide polymorphism (SNP) and 9117 silicoDArT markers. Genotypic data were cleaned for redundant and non-polymorphic markers, markers with switched alleles, markers with ≥50% missing data and significantly distorted markers ($p < 0.05$) in RStudio version 1.1.463 [56] and JoinMap® version 4.1 [57]. A total of 483 SNP and silicoDArT polymorphic markers were used to construct a genetic map for the Tugela-Dn × Elands mapping population, while 1144 silicoDArT markers formed a genetic linkage map for the Elands × Flamink mapping population. The order of markers within a linkage group was established based on a regression mapping algorithm [58]. Map distances (cM) were calculated from recombination frequencies using the Kosambi mapping function [59].

2.5. QTL Analysis

QTL analysis was performed using Windows QTL Cartographer version 2.5 [60]. Composite interval mapping (CIM) was used to screen for significant QTLs using individual mean scores per environment and average mean scores across all environments. QTL detection was based on 1000 permutations ($\alpha = 0.05$). The forward regression model was used with a window size of 10 cM, a walk speed of 2 cM and five control markers. QTLs were named following the international rules of genetic nomenclature adapted for wheat [61].

3. Results

3.1. Phenotypic Performance of Genotypes and Parents across Multi-Environments

The performance of genotypes in the six environments was depicted through histograms (frequency distribution, Figure 1) and an AMMI biplot (genotype stability, Figure 2). Both the Shapiro–Wilk test ($p < 0.001$) and Wilcoxon matched-pairs test ($p < 0.001$) proved the non-normality of PHS tolerance in some study environments. However, the results of the ANOVA and Kruskal–Wallis test were almost similar, suggesting less variation between variables. Significant differences among the three parents, one-hundred and ninety-four genotypes and six environments were observed (Table 2). The genotype × environment interaction, which was estimated from the error mean square (MSge) of the replicated parents according to an augmented design defined by Federer [54] was significant for PHS tolerance. Among the parents, Elands was PHS-tolerant (score of 2.00) and Flamink was moderately tolerant (score of 3.40), while Tugela-Dn displayed a susceptible reaction to PHS (score of 5.00) (Figure 1, Table 3). As expected, on average, the frequency distribution of genotypes was continuous (Figure 1), indicating the presence of transgressive segregation, with some individuals exhibiting higher or lower PHS tolerance scores than the parents.

This observation suggested polygenic control. A broad-sense heritability estimate of 0.5414 was calculated for DH lines (Table 2).

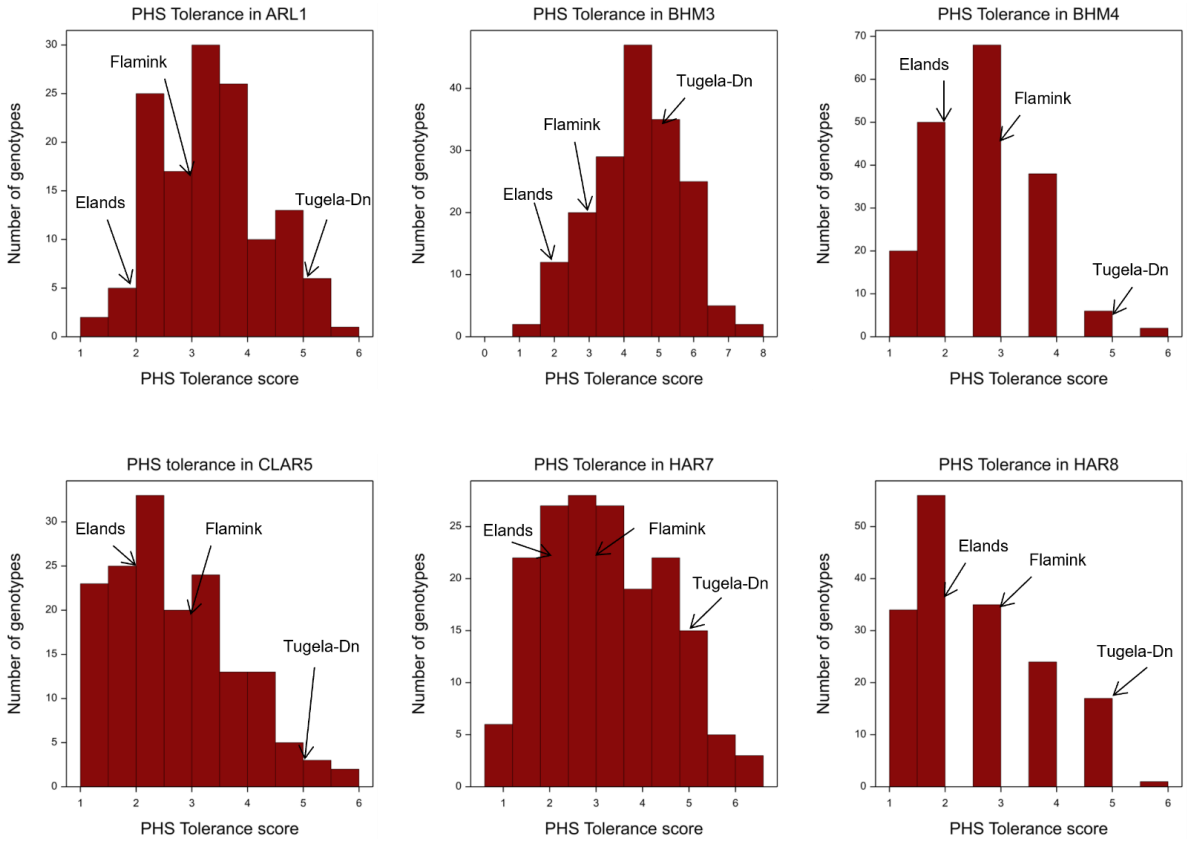

Figure 1. Frequency distribution of DH lines and parents for PHS tolerance in the six environments.

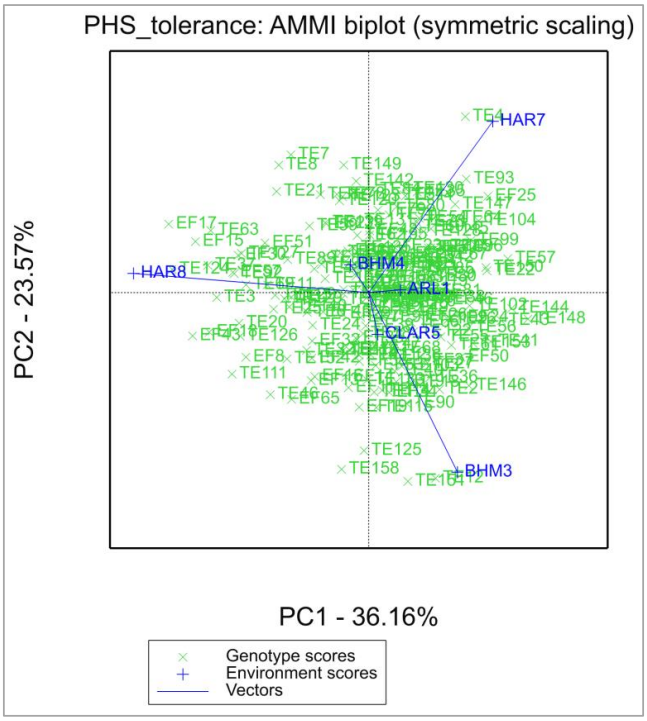

Figure 2. The AMMI biplot for PHS tolerance illustrating patterns of genotype × environment interaction and genotype stability across six environments.

Table 2. Mean squares and the broad-sense heritability (H^2) estimate of PHS tolerance in 194 DH lines and 3 parents across 6 environments.

Source of Variation	Degrees of Freedom	Mean Square	F (*p*-Value)
Parents	2	84.873	<0.001
Environment	5	5.434	<0.001
Replications	4	1.861	
Parents × Environment	9	1.580	0.017
Residual	56	0.627	
Genotypes	193	2.429	<0.001
Environment	5	74.182	<0.001
Replications			
Genotype × Environment	799	1.114	0.017
H^2		0.5414	
H^2 (%)		54.14	

Table 3. PHS tolerance scores of the top ten best- and five worst-performing DH lines and parents across the six environments to highlight the overall performance of the two DH populations.

† Genotype/Parent	‡ Environment						Average PHS Tolerance Score
	ARL1	BHM3	BHM4	CLAR5	HAR7	HAR8	
PHS tolerance scores of the top ten best-performing DH lines							
EF 44	*	2	1	2	2	1	1
EF 15	*	2	2	1	1	4	2
EF 17	*	2	1	1	2	5	2
EF 47	*	4	1	1	1	1	2
TE 21	1	2	2	1	3	3	2
TE 37	2	2	2	2	1	4	2
TE 62	2	2	4	2	2	1	2
TE 73	2	3	2	1	3	1	2
TE 122	2	4	1	1	2	1	2
TE 127	1	3	2	2	2	4	2
PHS tolerance scores of the top five worst-performing DH lines							
TE 48	4	6	4	2	5	5	4
TE 145	5	4	5	4	5	2	4
TE 67	5	6	4	4	6	3	5
TE 149	5	5	6	5	6	5	5
TE 155	4	6	3	4	6	5	5
PHS tolerance scores of the three parental cultivars							
Tugela-Dn	4	6	5	5	5	5	5
Elands	2	3	2	1	2	2	2
Flamink	*	5	3	3	4	2	3.4

† Genotype denotes a DH line. TE denotes a Tugela-Dn × Elands DH line, while EF denotes an Elands × Flamink DH line. Parent denotes the three parental cultivars, i.e., Elands, Flamink and Tugela-Dn. ‡ Environment denotes ARL1 for Arlington 2016, BHM3 for Bethlehem 2016, BHM4 for Bethlehem 2017, CLAR5 for Clarens 2016, HAR7 for Harrismith 2016 and HAR8 for Harrismith 2017. * denotes missing data.

Two principal components of the AMMI biplot, PC1 = 36.16% and PC2 = 23.57%, explained the observed phenotypic variation in genotypes across environments (Figure 2). Less genotype × environment interactions (indicated by the length of vectors) were observed in ARL1, BHM4 and CLAR5 in contrast to BHM3, HAR7 and HAR8. Most DH lines were found clustered toward the centre of the biplot, proving broad adaptation and good performance. The average performance of DH lines across environments followed the order HAR8 (most tolerant) > CLAR5 > BHM4 > HAR7 > ARL1 > BHM3 (least tolerant), with PHS tolerance scores ranging from 3.00 to 4.00. These observations suggest tolerant to moderate

reactions of the two DH populations. DH lines exhibited PHS tolerance scores ranging from 1.00 to 8.00, with an average score of 3.19 ± 1.32. (mean ± standard deviation).

3.2. Selection of Best-Performing Genotypes

On average, most (62.37%) DH lines had PHS tolerance scores ≤ 3.00 (from a scale of 1 to 8, Figure S1, Table S1), indicating the tolerance of the two populations to PHS [15]. About 16.50% of DH lines performed to the level of Elands (the PHS-tolerant parent), with PHS tolerance scores ≤ 2.00, and are recommended for further selection in a pre-breeding or breeding programme. Table 3 shows the PHS tolerance scores of the best-performing DH lines (represented by the top ten) in contrast to the parents across the six environments. Poorly performing DH lines similar to Tugela-Dn (the PHS-susceptible parent with a score of 5.00) are also represented by the top five worst-performing genotypes in Table 3. The overall phenotypic data of the 194 DH lines and the 3 parents across the 6 environments are provided as supplementary data (Table S1).

3.3. Genetic Linkage Map Construction

Genetic maps of the two DH populations, Tugela-Dn × Elands and Elands × Flamink, were constructed using different marker sets genotyped with the DArT-sequencing genotype-by-sequence (GBS) platform 1.0 (DArT, Pty Ltd., Yarralumla, ACT, Australia). Many markers, however, with a high level of missing data, had been used to genotype the Tugela-Dn × Elands population. For the quality and reliability of the results, only 483 polymorphic markers with ≥50% of genotypic data were used for genetic map construction of the Tugela-Dn × Elands population, and both parents share "SA1684" in their pedigrees, which resulted in fewer markers mapped per chromosome. The high level of missing data is usually the case with DArTseq GBS SNPs and a major concern for further applications, such as QTL mapping [62–64]. This is due to the low sequencing coverage that significantly reduces the number of usable SNPs, lower marker density and the resulting linkage map density [65,66].

The 483 polymorphic markers consisted of an ALMT1-4 functional marker pair, 259 SNP markers and 223 silicoDArT markers. Twenty-three linkage groups (LG) were identified representing the twenty-one wheat chromosomes. The entire genetic map spanned 1516.57 cM of the wheat genome, with an average distance of 3.87 cM between adjacent markers (Table 4). Genetic distances between adjacent markers ranged from 0.58 cM on chromosome 6BLG1 to 8.71 cM on chromosome 3DLG2. The number of markers on each chromosome varied between 7 on 3D.LG2 and 6D and 40 on 2B. More (51.76%) markers mapped to the B sub-genome, followed by the A sub-genome (24.84%), and the lowest number (23.40%) of markers was observed on the D sub-genome. The distribution of markers in the three sub-genomes of the bread wheat genome is comparable to the observation of Cabral et al. [30]. The A, B and D sub-genomes covered total lengths of 480.77 cM, 588.92 cM and 446.88 cM, respectively.

A total of 1144 polymorphic silicoDArT markers were used to construct the genetic map for the Elands/Flamink mapping population. The genetic map represented all 21 wheat chromosomes and covered a length of 311.59 cM of the wheat genome, with an average distance of 0.27 cM between adjacent markers (Table 4). The number of markers on each chromosome varied between 11 on 4B and 83 on 2A. Chromosomes 3D and 6B had the highest marker density of 0.20 cM, while 4A showed the lowest marker density of 1.21 cM. The A sub-genome was the longest with 107.59 cM (34.88% of markers), followed by the B sub-genome with 103.25 cM (29.02% of markers), and the shortest was the D sub-genome with 100.75 cM (36.10% of markers).

Denser linkage maps (with an average distance of 0.27 cM between adjacent markers) were formed with the Elands × Flamink mapping population in contrast to the Tugela-Dn × Elands mapping population (with an average distance of 3.87 cM between adjacent markers). Only 18 (silicoDArT) markers shared and maintained the marker order similarity (1.11%) between linkage maps of the two mapping populations. Most common

markers between the two genetic maps lacked polymorphism, were significantly distorted ($p < 0.05$) and suffered from high missing data rates and heterozygote under-calling. Consequently, such (less informative) markers were removed in the filtering process before linkage analyses.

Table 4. Genetic linkage maps showing marker distribution in the 21 wheat chromosomes in Tugela-Dn × Elands and Elands × Flamink mapping populations.

	Tugela-Dn × Elands Linkage Map				Elands × Flamink Linkage Map			
LG †	**Chrom ‡**	**No. of Markers**	**Map Length (cM)**	**Marker Density (cM)**	**Chrom ‡**	**No. of Markers**	**Map Length (cM)**	**Marker Density (cM)**
1	1A	19	49.33	2.60	1A	67	19.96	0.30
2	1B	30	90.05	3.00	1B	81	19.76	0.24
3	1D	25	76.50	3.06	1D	51	21.69	0.43
4	2A	17	96.05	5.65	2A	83	17.76	0.21
5	2B	40	75.98	1.90	2B	57	13.63	0.24
6	2D	11	73.56	6.69	2D	56	12.02	0.21
7	3A	8	49.80	6.22	3A	79	20.89	0.26
8	3B	29	58.84	2.03	3B	64	14.45	0.23
9	3D.LG1	8	28.95	3.62	3D	59	11.84	0.20
10	3D.LG2	7	60.95	8.71	4A	25	9.38	0.38
11	4A	8	48.35	6.04	4B	11	13.29	1.21
12	4B	23	82.90	3.60	4D	53	14.07	0.27
13	4D	15	74.35	4.96	5A	72	15.64	0.22
14	5A	14	53.35	3.81	5B	47	13.89	0.30
15	5B	31	76.91	2.48	5D	67	14.47	0.22
16	5D	15	34.15	2.28	6A	31	11.78	0.38
17	6A	20	57.27	2.86	6B	32	15.27	0.48
18	6B.LG1	31	17.90	0.58	6D	59	11.61	0.20
19	6B.LG2	27	75.70	2.80	7A	42	12.18	0.29
20	6D	7	55.74	7.96	7B	40	12.97	0.32
21	7A	34	126.62	3.72	7D	68	15.07	0.22
22	7B	39	110.63	2.84				
23	7D	25	42.67	1.71				
	A sub-genome	120	480.77	4.01	A sub-genome	399	107.59	0.27
	B sub-genome	250	588.92	2.36	B sub-genome	332	103.25	0.31
	D sub-genome	113	446.88	3.96	D sub-genome	413	100.75	0.24
	Total Genome	483	1516.57	3.87	Total Genome	1144	311.59	0.27

† LG denotes linkage group. ‡ Chrom denotes chromosome.

A low marker/map density was observed due to the low sequencing coverage of DArTseq markers [65,66] and the narrow genetic basis as both Tugela-DN and Elands share "SA1684" in their pedigrees [49], and also a limited number of crossing-over events in one population's linkage maps [67,68]. All these factors contributed to the observed low marker similarity between linkage maps of the two mapping populations. Marker imputation, genotyping using highly polymorphic markers and diverse populations or other next-generation sequencing-based marker platforms such as SNP Arrays and crop-specific exome capture technologies, or the use of a consensus genetic map, can be expected to enhance the linkage analysis results in a further study [62,63,68,69].

3.4. QTL Mapping Analysis

3.4.1. Additive QTLs Detected in the Tugela-Dn × Elands Mapping Population

A total of 14 additive QTLs for PHS tolerance were detected across six environments in the Tugela-Dn × Elands mapping population (Table 5). Three QTLs were detected in more than one environment and were considered to be stable. Stable QTLs for PHS tolerance were identified on chromosomes 5B and 7B and explained a phenotypic variation (PVE) varying between 10.08% and 20.30%, with LOD scores ranging from 2.73 to 3.11. Elands (PHS-tolerant parent) contributed a greater (83.33%) additive effect than Tugela-Dn (PHS-susceptible parent) to the mapped stable QTLs.

Table 5. Additive QTLs for PHS tolerance detected in Tugela-Dn × Elands and Elands × Flamink DH mapping populations across six environments. QTL effects are only shown for environments with detected QTLs (√).

QTLs Mapped in the Tugela-Dn × Elands DH Mapping Population															
Trait	**Nearby Marker**	**Position [a]**	**QTL [b]**	**Detected Environments [c]**								**QTL Effects [d]**			
				ARL1	**BHM3**	**BHM4**	**CLAR5**	**HAR7**	**HAR8**	**AVE**	**LOD**	**Add**	**PVE (%)**	**LOD**	**Add**	**PVE (%)**
PHS	**4910940 | F | 0–22:A > G; 4395011 | F | 0–8:T > C**	**5B (28–29)**	***QPhs.sgi-5B.3*$^{+}$**	¥	¥	√	¥	¥	√	¥	**3.11**	**0.33**	**10.08**	**3.01**	**−0.45**	**11.56**
	5582828 | F | 0–6:C > T; 3024652 | F | 0–22:C > T	**7B (60–66)**	***QPhs.sgi-7B.4*$^{+}$**	¥	¥	¥	√	√	¥	¥	**3.10**	**−0.52**	**20.30**	**2.85**	**−0.49**	**11.89**
	3021324 | F | 0–20:T > C; 6041508 | F | 0–33:G > T	**7B (100–101)**	***QPhs.sgi-7B.2*$^{+}$**	¥	√	√	¥	¥	¥	¥	**2.76**	**−0.48**	**10.66**	**2.73**	**−0.36**	**11.00**
	7329308	7B (11)	*QPhs.sgi-7B.1*	¥	√	¥	¥	¥	¥	¥	3.21	0.51	10.97	¥	¥	¥
	3025468 | F | 0–18:T > G; 12343039 | F | 0–26:G > T	3B (7)	*QPhs.sgi-3B*$^{+}$	¥	¥	¥	√	¥	¥	√	3.87	−0.40	11.49	4.09	−0.23	11.92
	4394765 | F | 0–8:C > G; 1684411 | F | 0–9:G > T	7A (30–64)	*QPhs.sgi-7A*$^{+}$	¥	¥	¥	¥	¥	√	√	3.80	0.69	28.75	5.85	0.29	18.41
	5050436 | F | 0–32:T > C	1A (20)	*QPhs.sgi-1A*	¥	¥	√	¥	¥	¥	¥	4.63	−0.42	14.19	¥	¥	¥
	1082843 | F | 0–43:T > C	1B (22)	*QPhs.sgi-1B*	¥	¥	¥	¥	√	¥	¥	2.56	−0.53	16.97	¥	¥	¥
	5582507 | F | 0–13:C > G	2A (90)	*QPhs.sgi-2A*	√	¥	¥	¥	¥	¥	¥	3.66	−0.33	11.06	¥	¥	¥
	5324489; 5324039	2B (45–53)	*QPhs.sgi-2B.2*	¥	√	¥	¥	¥	¥	¥	2.92	−0.49	8.15	¥	¥	¥
	3029334 | F | 0–25:C > G	3DLG2 (4)	*QPhs.sgi-3DLG2*	¥	¥	¥	¥	¥	¥	√	2.52	0.27	16.03	¥	¥	¥
	4395594 | F | 0–22:T > C	5B (38)	*QPhs.sgi-5B.1*	√	¥	¥	¥	¥	¥	¥	4.12	0.36	12.96	¥	¥	¥
	3064906 | F | 0–10:T > A	5B (44)	*QPhs.sgi-5B.2*	√	¥	¥	¥	¥	¥	¥	3.78	0.47	22.63	¥	¥	¥
	1268172 | F | 0–33:C > G	6B.LG2 (4)	*QPhs.sgi-6BLG2*	¥	√	¥	¥	¥	¥	¥	3.46	−0.53	12.78	¥	¥	¥
QTLs Mapped in the Elands × Flamink DH Mapping Population															
PHS	3029487	2D (0)	*QPhs.sgi-2D*	¥	¥	¥	¥	√	¥	¥	3.51	−1.29	21.84	¥	¥	¥

[a] Position indicates the chromosome and exact position (in cM) at which the QTL was mapped. [b] QTLs are denoted according to McIntosh et al. (2003). QTL significance was tested at $p = 0.05$, LOD = 2.5. √ denotes a QTL detected, and ¥ denotes a lack of QTLs. [c] Detected environments denotes ARL1, Arlington 2016; BHM3, Bethlehem 2016; BHM4, Bethlehem 2017; CLAR5, Clarens 2016; HAR7, Harrismith 2016; HAR8, Harrismith 2017. "AVE" indicates the combined QTL analysis based on average PHS tolerance scores across all six environments. [d] QTL effects describe the logarithm of the odds (LOD) score; the additive effect (Add); and the phenotypic variation explained by the QTLs in percentage (PVE (%)). In the Tugela-Dn × Elands population, a negative additive effect shows that contributing alleles were from Elands, and a positive effect indicates an influence from Tugela-Dn. In the Elands × Flamink population, a negative additive effect shows an influence from Elands, while a positive effect indicates an influence from Flamink. + and bold indicate QTLs shared between at least two environments.

3.4.2. Additive QTLs Detected in the Elands × Flamink Mapping Population

A single additive, although unstable, QTL for PHS tolerance was detected in HAR7 using the Elands × Flamink mapping population (Table 5). This QTL was mapped on chromosome 2D. Consequently, there were no putative stable QTLs shared between the two genetic backgrounds.

4. Discussion

4.1. Phenotypic Variations Attributed to Environmental Differences

The results of the transgressive segregation, the AMMI biplot and ANOVA reveal significant effects of genotypes, environments and the genotype × environment interaction on PHS tolerance. These phenotypic variations underscored the complex genetic control and the strong influence of the environment on the expression of PHS tolerance [70–74]. Environmental factors such as temperature, relative humidity and rainfall received during the grain filling and maturation stages of wheat greatly impact PHS tolerance [5,27,75]. The six study environments differed in average daily temperatures, humidity and rainfall received between the grain filling, maturity and harvest stages of wheat over the 2016 and 2017 planting seasons (Table 1). These could explain the observed variation in the PHS response of genotypes (Figures 1 and 2, Tables 3 and S1).

Cool temperatures (low humidity) retain seed dormancy, whilst high temperatures during the later stages of grain development can break embryo dormancy, thus increasing the chances of PHS occurrence if rain (more than 15–20 mm) occurs around harvest time [75–77]. Higher average daily humidity coupled with high average daily temperatures

and rainfall was observed in BHM3 between the grain filling and harvest stages of wheat (October 2016–January 2017, Table 1). These conditions could explain the higher PHS scores (average of 4.40) recorded in this environment. On the contrary, ARL1 was the driest with high average daily temperatures, low average daily humidity and almost no rainfall and yielded moderately resistant PHS scores (average of 3.30).

The other environmental (CLAR5, HAR7 and BHM4) conditions were average and almost invariable with the average daily temperature range of 24–27 °C, humidity of 84–93% and rainfall of 1.22–5.54 mm (Table 1). These environmental conditions are reportedly favourable for growing winter wheat [78], which could explain the good performance of genotypes observed in these environments in comparison to ARL1 and BHM3. These observations concur with the phenotypic analysis results which ranked the average performance of DH lines across environments in the following order: HAR8 (most tolerant) > CLAR5 > BHM4 > HAR7 > ARL1 > BHM3 (least tolerant).

Nonetheless, wheat-producing regions in South Africa remain prone to PHS attributed to high temperatures coupled with summer rainfall that occur around the harvesting season [19]. This makes breeding for PHS tolerance a main target in these and other regions for the improvement in grain yield and quality [43,44,46]. The results of this study indicate that the DH lines possess great phenotypic variation (ANOVA), stability across environments (AMMI biplot) and tolerance to PHS. These observations corroborate the QTL mapping of PHS tolerance to facilitate the improvement in wheat grain yield and end-use quality through marker-assisted selection (MAS).

4.2. QTL Mapping Analysis of PHS Tolerance

QTLs detected in more than one of the six environments were considered stable, and the PVE of ≥10% signified loci of major effects [79]. Three stable additive QTLs of major effects were detected for PHS tolerance through the Tugela-Dn × Elands mapping population (Table 5). These loci are population-specific (QTL × genetic background interaction) as they could not be detected in the Elands × Flamink genetic background. However, both populations exhibited a resistant to moderate phenotype across environments (Figures 1 and 2, Tables 3 and S1). The observed tolerance could prove the strong and dominant (PHS-tolerant) effect of Elands as the common parent between the two populations. Failure to detect the associated genomic regions in both genetic backgrounds may be attributed to various internal and external factors affecting the gene expression [5,27].

Potential factors for the lack of detection of common PHS tolerance loci in both genetic backgrounds may include the observed low marker and map densities, especially in the Tugela-Dn × Elands genetic map (Table 4, average marker density of 3.87 cM). This may have affected the power of QTL detection in the Windows QTL Cartographer statistical software used [80]. However, high-density maps have been shown to neither improve the QTL detection power nor the predictive power for the proportion of explained genotypic variance, but to improve the precision of QTL localisation and estimated QTL effects, especially for the detected minor QTLs, as well as the power to resolve closely linked QTLs [81,82]. Another possible reason for the lack of shared QTLs between the two mapping populations may be the lack of polymorphic silicoDArT markers for PHS tolerance in the constructed genetic map for the Elands × Flamink population. This was evident in that the three genomic regions identified for PHS tolerance in the Tugela-Dn × Elands population were all signalled by SNP markers (Table 5). It may also happen that the environmental conditions were not favourable enough for PHS detection in some environments, which could affect QTL detection in both genetic backgrounds. PHS tolerance has proven to be a complex trait highly influenced by environmental conditions [5], which concurred with the ANOVA results (Table 2). Stable genomic regions influencing PHS tolerance were identified on chromosomes 5B within a 28–29 cM interval (designated *QPhs.sgi-5B.3*$^{+}$) and 7B within a 60–101 cM interval (designated *QPhs.sgi-7B.2*$^{+}$ and *QPhs.sgi-7B.4*$^{+}$) (Table 5). The well-known PHS-tolerant parent, Elands [52], was the main donor of favourable alleles in two (*QPhs.sgi-7B.2*$^{+}$ and *QPhs.sgi-7B.4*$^{+}$) of the three stable loci identified. Both

Elands and the PHS-susceptible parent, Tugela-Dn, co-influenced *QPhs.sgi-5B.3*$^{+}$. The observed resistant to moderate phenotype in the Tugela-Dn × Elands population across environments was, therefore, presumed to be mainly conditioned by these three loci of major effects (PVE = 10.08–20.30%, LOD = 2.73–3.11).

The three genomic regions reported in the present study signify progress in the identification and validation of genomic regions influencing PHS tolerance in the South African bread wheat material. This proves genotypic variation in PHS tolerance in the SA wheat cultivars, which has been mainly achieved through conventional breeding [20,23], considering the recent incorporation of molecular markers in breeding for PHS tolerance in wheat in the country [25]. The three identified loci have shown some stability and potential usefulness in conferring tolerance to PHS in the tested SA environment. This requires further validation; however, these findings are anticipated to facilitate the on-going breeding efforts for PHS tolerance, which will enable the development of PHS-tolerant cultivars adapted to the SA environment.

Our study results are comparable to the findings of other studies conducted in different environments, which have reported >250 QTLs associated with PHS tolerance on all 21 wheat chromosomes using diverse mapping populations [6]. Gupta et al. [6] reported that, up to date, there are 29 stable major QTLs for PHS tolerance distributed on 12 different chromosomes, including 1B, 2B, 2D, 3A, 3B, 3D, 4A, 4B, 5A, 6A, 7B and 7D. The findings of Gupta et al. [6], Lin et al. [83] and Martinez et al. [4] are comparable to the stable QTLs for PHS tolerance identified on chromosome 7B in the present study. Cao et al. [33] also reported a QTL conferring early heading, a trait indirectly influencing PHS tolerance on chromosome 7B, in the vicinity of the *Vrn-B3* locus.

In another study aimed to identify candidate genes, regions and markers for PHS resistance in wheat, Cabral et al. [30] identified genomic regions (QTLs and candidate genes through comparative mapping) associated with PHS resistance on chromosome 7B in wheat, brachypodium and rice. *QPhs.sgi-7B.4*$^{+}$ identified on the 60–66 cM interval of chromosome 7B in the present study can compare to the genomic region (55.6–59.5 cM) identified by Cabral et al. [30]. Pending further validation, this is anticipated to be the same QTL mapped by Cabral et al. [30] as both genomic regions accounted for 11.8–20% of the PVE. *QPhs.sgi-7B.2*$^{+}$ was mapped on 100–101 cM and explained 10.66–11.00% of the PVE, suggesting it is a different QTL. *QPhs.sgi-5B.3*$^{+}$ identified on chromosome 5B (28–29 cM) in the present study can compare to the findings of Singh et al. [84] and Fofana et al. [85]. In addition, Zhou et al. [86] identified a stable minor QTL (PVE = 4.36–5.94%) associated with PHS resistance on chromosome 5BS, which can compare to *QPhs.sgi-5B.3*$^{+}$ (PVE = 10.08–11.56%). These comparable studies were conducted in the United States [4,83], Japan [33], Canada [30,84,85] and China [86], in contrast to our South African environment. This proves the validity of these results.

Chromosomes 1A, 1D, 2D, 3A, 3B, 3D, 4A, 5A, 6B and 7A harboured potential loci for PHS tolerance; however, they were detected only in single environments in the present study. Chromosome 2B and the above-mentioned chromosomes have repeatedly been reported to harbour stable loci of minor and major effects for PHS tolerance in various studies [30,32,40,72,83,87–90]. These studies highlighted the importance of these chromosomes in the improvement in PHS tolerance, grain yield-related traits and other agronomic traits of importance. Consequently, some major QTLs have been validated and fine-mapped [30,32], and the underlying candidate genes have been cloned [29,91] and are useful in MAS for the continued improvement in wheat grain yield and quality.

The QTL analysis results of our study attest that the inability to consistently detect stable QTLs for PHS tolerance across all study environments does not necessarily mean that they are not present, but that the expression of the genotype's tolerance (favourable alleles) depends upon many factors [27,72,74]. Firstly, the environmental variation (temperature, humidity and rainfall), whose effect was tested through ANOVA (Table 2) and found to be significant ($p < 0.001$) in the present study, could modify the effects of alleles contributing to the genotype's tolerance to PHS [40,75]. Secondly, the expression of the genotype's

tolerance to PHS is influenced by the genotype × environment interaction, which was found to be significant (p = 0.017, Table 2) in the present study, suggesting variable genetic effects in different environments [92]. Favourable alleles are not readily expressed until triggered by favourable (continuous rainy and humid) weather conditions prior to or during harvest [1,2]. Similarly, some weather conditions may suppress the expression and, therefore, the detection of PHS tolerance QTLs. Lin et al. [83] also observed inconsistency in the expression of stable QTLs for PHS tolerance across eight environments, which included both greenhouse and field experiments. Lin et al. [83] proved that the expression of other major stable QTLs is suppressed in the presence of extremely high temperatures in the field. These findings are comparable to our results as diverse weather conditions were observed in the six study environments (Table 1).

Thirdly, the low broad-sense heritability (H^2 = 54.14%, Table 2), which was estimated from genotypes, proved that more influence came from environmental factors influencing PHS tolerance. These and other factors significantly influence the expression and detection of PHS tolerance QTLs across environments, which could explain the inconsistencies observed with the detected stable QTLs and their estimated QTL effects in the present study.

Mapping stable loci in different environments and over years (and even better in different genetic backgrounds) is crucial in MAS as it validates the presence, position and effect of that QTL [93,94]. For example, locus *QPhs.sgi-7B.2*$^+$ that was mapped on chromosome 7B within the 100–101 cM interval was detected from the same locality (Bethlehem) over two consecutive years (2016 and 2017). The two other stable loci mapped on chromosomes 5B (*QPhs.sgi-5B.3*$^+$) and 7B (*QPhs.sgi-7B.4*$^+$) were each detected in the same year, but in different localities. This proves the reliability of the three stable loci for PHS tolerance identified in the present study. A detected QTL may disappear after marker-assisted introgression if it was a false positive or if its effect (expression) is highly influenced by either the QTL × QTL interaction, the QTL × genetic background interaction or the QTL × environment interaction [95,96]. The three stable QTLs identified for PHS tolerance have the potential to facilitate the on-going improvement in PHS tolerance in winter wheat.

5. Conclusions

The main aim of the present study was successfully executed. About 16.50% of DH lines performed to the level of Elands (the PHS-tolerant parent) and are recommended for further selection in a pre-breeding or breeding programme. Three genomic regions influencing PHS tolerance in winter bread wheat were identified on chromosomes 5B and 7B in the tested South African environment. These stable loci were detected in the Tugela-Dn × Elands genetic background and could not be validated in the Elands × Flamink genetic background. The results of this study validate previous findings that PHS is only expressed when environmental conditions are favourable, therefore providing a baseline for further validation of the detected loci. These findings are expected to expedite the on-going improvement in PHS tolerance in winter wheat, which will facilitate the development of PHS-tolerant cultivars adapted to the SA environment.

Supplementary Materials: The following supporting information can be downloaded at: https://www.mdpi.com/article/10.3390/agronomy12040832/s1, Figure S1: Rating scale (1–8) used to assign a PHS tolerance or susceptible score to the studied material [15]; Table S1: PHS tolerance scores of the 194 DH lines across the six environments.

Author Contributions: Conceptualisation, T.P.K. and T.J.T.; development of plant material, T.H. and T.J.T.; methodology, T.P.K., A.B. and T.J.T.; formal analysis, T.P.K.; investigation, T.P.K.; writing—original draft preparation, T.P.K.; writing—review and editing, T.P.K., T.H., A.B. and T.J.T.; supervision, A.B. and T.J.T.; funding acquisition, T.P.K. and T.J.T. All authors have read and agreed to the published version of the manuscript.

Funding: This research project was funded by the Agricultural Research Council–Small Grain (ARC-SG) and the National Research Foundation (NRF).

Institutional Review Board Statement: The study did not require ethical approval.

Informed Consent Statement: Not applicable.

Data Availability Statement: The data used in this study are available in supplementary material and the genomic data files are copyright and only available on request from the corresponding author.

Acknowledgments: Tebogo Oliphant is acknowledged for co-developing the two DH populations used in this study. The ARC-SG technical staff is thanked for assisting with field trials. Khashief Soeker (ARC-Infruitec-Nietvoobij, Stellenbosch, SA) and John Baison (RAGT Seeds Ltd., UK) are appreciated for their valuable assistance with JoinMap. The Mvelase family (Bergville, KZN, SA) and Mzungezi "Slavit" Mthembu (UKZN, SA) are greatly thanked for providing essential resources for writing the manuscript.

Conflicts of Interest: The authors declare no conflict of interest.

References

1. Groos, C.; Gay, G.; Perretant, M.R.; Gervais, L.; Bernard, M.; Dedryver, F.; Charmet, G. Study of the relationship between pre-harvest sprouting and grain colour by quantitative trait loci analysis in a white × red grain bread-wheat cross. *Theor. Appl. Genet.* **2002**, *104*, 39–47. [CrossRef]
2. Rodriguez, M.V.; Barrero, J.M.; Corbineau, F.; Gubler, F.; Benech-Arnold, R.L. Dormancy in cereals (not too much, not so little): About the mechanisms behind this trait. *Seed Sci. Res.* **2015**, *25*, 99–119. [CrossRef]
3. Mares, D.; Mrva, K.; Cheong, J.; Williams, K.; Watson, B.; Storlie, E.; Sutherland, M.; Zou, Y. A QTL located on chromosome 4A associated with dormancy in white- and red-grained wheats of diverse origin. *Theor. Appl. Genet.* **2005**, *111*, 1357–1364. [CrossRef] [PubMed]
4. Martinez, S.A.; Godoy, J.; Huang, M.; Zhang, Z.; Carter, A.H.; Garland, C.K.A.; Steber, C.M. Genome-wide association mapping for tolerance to preharvest sprouting and low falling numbers in wheat. *Front. Plant Sci.* **2018**, *9*, 141. [CrossRef] [PubMed]
5. Ali, A.; Cao, J.; Jiang, H.; Chang, C.; Zhang, H.P.; Sheikh, S.W.; Shah, L.; Ma, C. Unraveling molecular and genetic studies of wheat (*Triticum aestivum* L.) resistance against factors causing pre-harvest sprouting. *Agronomy* **2019**, *9*, 117. [CrossRef]
6. Gupta, P.K.; Balyan, H.S.; Sharma, S.; Kumar, R. Genetics of yield, abiotic stress tolerance and biofortification in wheat (*Triticum aestivum* L.): A review. *Theor. Appl. Genet.* **2020**, *133*, 1569–1602. [CrossRef]
7. Andreoli, C.; Bassoi, M.C.; Brunetta, D. Genetic control of seed dormancy and pre-harvest sprouting in wheat. *Sci. Agric.* **2006**, *63*, 564–566. [CrossRef]
8. Simsek, S.; Ohm, J.B.; Lu, H.; Rugg, M.; Berzonsky, W.; Alamri, M.S.; Mergoum, M. Effect of pre-harvest sprouting on physico-chemical properties of starch in wheat. *Foods* **2014**, *3*, 194–207. [CrossRef]
9. Ponce-García, N.; Ramírez-Wong, B.; Escalante-Aburto, A.; Torres-Chávez, P.I.; Serna-Saldivar, S.O. Grading factors of wheat kernels based on their physical properties. In *Wheat Improvement, Management and Utilization*; Wanyera, R., Owuoche, J., Eds.; IntechOpen: London, UK, 2017; pp. 275–291. [CrossRef]
10. Gavazza, M.I.A.; Bassoi, M.C.; Carvalho, T.C.; de Bespalhok, F.J.C.; Panobianco, M. Methods for assessment of pre-harvest sprouting in wheat cultivars. *Pesqui. Agropecuária Bras.* **2012**, *47*, 928–933. [CrossRef]
11. Depauw, R.M.; Hucl, P.; Knox, R.E.; Singh, A.K.; Fox, S.L.; Humphreys, D.G. Developing standardized methods for breeding preharvest sprouting resistant wheat, challenges and successes in Canadian wheat. *Euphytica* **2012**, *188*, 7–14. [CrossRef]
12. Olaerts, H.; Courtin, C.M. Impact of preharvest sprouting on endogenous hydrolases and technological quality of wheat and bread: A review. *Compr. Rev. Food Sci. Food Technol.* **2018**, *17*, 698–713. [CrossRef] [PubMed]
13. Food and Agriculture Organization of the United Nations (FAO). *The Future of Food and Agriculture—Alternative Pathways to 2050*; Summary Version; FAO: Rome, Italy, 2018; 60p.
14. Ben Mariem, S.; Soba, D.; Zhou, B.; Loladze, I.; Morales, F.; Aranjuelo, I. Climate Change, Crop Yields, and Grain Quality of C_3 Cereals: A Meta-Analysis of [CO_2], Temperature, and Drought Effects. *Plants* **2021**, *10*, 1052. [CrossRef] [PubMed]
15. Barnard, A.; Purchase, J.L.; Smith, M.F.; van Lill, D. Determination of the preharvest sprouting resistance of South African winter wheat (*Triticum aestivum* L.) cultivars. *S. Afr. J. Plant Soil* **1997**, *14*, 4–8. [CrossRef]
16. Van Niekerk, H.A. Southern Africa Wheat Pool. In *The World Wheat Book: The History of Wheat Breeding*; Bonjean, A.P., Angus, W.J., Eds.; Lavoisier Publishing: Paris, France, 2001; pp. 923–926.
17. Barnard, A.; Bona, L. Sprout damage and falling number in South African and Hungarian wheats. *Cereal Res. Commun.* **2004**, *32*, 259–264. [CrossRef]
18. Barnard, A.; Smith, M.F. The effect of rainfall and temperature on the preharvest sprouting tolerance of winter wheat in the dryland production areas of the Free State Province. *Field Crops Res.* **2009**, *112*, 158–164. [CrossRef]
19. Sydenham, S.L.; Barnard, A. Targeted haplotype comparisons between South African wheat cultivars appear predictive of pre-harvest sprouting tolerance. *Front. Plant Sci.* **2018**, *9*, 63. [CrossRef]
20. Barnard, A.; Grain, S.A. Preharvest Sprouting Research—20 Years Later. 2018. Available online: https://www.grainsa.co.za/preharvest-sprouting-research-20-years-later (accessed on 6 January 2022).

21. Barnard, A. Genetic diversity of South African winter wheat cultivars in relation to preharvest sprouting and falling number. *Euphytica* **2001**, *119*, 107–110. [CrossRef]
22. Craven, M.; Barnard, A.; Labuschagne, M.T. The impact of cold temperatures during grain maturation on selected quality parameters of wheat. *J. Sci. Food Agric.* **2007**, *87*, 1783–1793. [CrossRef]
23. Smit, H.A.; Tolmay, V.L.; Barnard, A.; Jordaan, J.P.; Koekemoer, F.P.; Otto, W.M. An overview of the context and scope of wheat (*Triticum aestivum*) research in South Africa from 1983 to 2008. *S. Afr. J. Plant Soil* **2010**, *27*, 81–96. [CrossRef]
24. Barnard, A.; Van Deventer, C.S.; Maartens, H. Genetic variability of preharvest sprouting in the South African situation. *Euphytica* **2005**, *143*, 291–296. [CrossRef]
25. ProAgri, SA. Wheat Production: The Use of Molecular Markers to Assist in Pre-Harvest Sprouting Research. 2016. Available online: https://www.proagri.co.za/en/wheat-production-use-molecular-markers-assist-pre-harvest-sprouting-research/ (accessed on 9 September 2021).
26. Johansson, E. Effect of two genotypes and Swedish environment on falling number, amylase activities, and protein concentration and composition. *Euphytica* **2002**, *126*, 143–149. [CrossRef]
27. Gao, X.; Hu, C.H.; Li, H.Z.; Yao, Y.J.; Meng, M.; Dong, J. Factors affecting pre-harvest sprouting resistance in wheat (*Triticum aestivum* L.): A review. *J. Anim. Plant Sci.* **2013**, *23*, 556–565.
28. Nornberg, R.; de Souza, L.H.; da Silva, J.A.G.; Zimmer, C.M.; Cima, F.F.; Olivo, M.; de Oliveira, A.C. The challenge of finding high grain yield and pre-harvest sprouting tolerant genotypes in Brazilian wheat germplasm. *Aust. J. Crop Sci.* **2016**, *10*, 977–984. [CrossRef]
29. Liu, S.; Sehgal, S.K.; Li, J.; Lin, M.; Trick, H.N.; Yu, J. Cloning and characterization of a critical regulator for preharvest sprouting in wheat. *Genetics* **2013**, *195*, 263–273. [CrossRef]
30. Cabral, A.L.; Jordan, M.C.; McCartney, C.A.; You, F.M.; Humphreys, D.G.; MacLachlan, R.; Pozniak, C.J. Identification of candidate genes, regions and markers for pre-harvest sprouting resistance in wheat (*Triticum aestivum* L.). *BMC Plant Biol.* **2014**, *14*, 340. [CrossRef]
31. Gao, F.; Wen, W.; Liu, J.; Rasheed, A.; Yin, G.; Xia, X. Genome-wide linkage mapping of QTL for yield components, plant height and yield-related physiological traits in the Chinese wheat cross Zhou 8425B/Chinese Spring. *Front. Plant Sci.* **2015**, *6*, 1099. [CrossRef]
32. Lin, M.; Cai, S.; Wang, S.; Liu, S.; Zhang, G.; Bai, G. Genotyping-by-sequencing (GBS) identified SNP tightly linked to QTL for pre-harvest sprouting resistance. *Theor. Appl. Genet.* **2015**, *128*, 1385–1395. [CrossRef]
33. Cao, L.; Hayashi, K.; Tokui, M.; Mori, M.; Miura, H.; Onishi, K. Detection of QTLs for traits associated with pre-harvest sprouting resistance in bread wheat (*Triticum aestivum* L.). *Breed. Sci.* **2016**, *66*, 260–270. [CrossRef]
34. Su, Z.; Jin, S.; Lu, Y.; Zhang, G.; Chao, S.; Bai, G. Single nucleotide polymorphism tightly linked to a major QTL on chromosome 7A for both kernel length and kernel weight in wheat. *Mol. Breed.* **2016**, *36*, 15. [CrossRef]
35. El-Feki, W.M.; Byrne, P.F.; Reid, S.D.; Haley, S.D. Mapping quantitative trait loci for agronomic traits in winter wheat under different soil moisture levels. *Agronomy* **2018**, *8*, 133. [CrossRef]
36. Guan, P.; Lu, L.; Jia, L.; Kabir, M.R.; Zhang, J.; Lan, T. Global QTL analysis identifies genomic regions on chromosomes 4A and 4B harboring stable loci for yield-related traits across different environments in wheat (*Triticum aestivum* L.). *Front. Plant Sci.* **2018**, *9*, 529. [CrossRef] [PubMed]
37. Zeeshan, M.; Arshad, W.; Khan, M.I.; Ali, S.; Nawaz, A.; Batool, A. Breeding for pre-harvest sprouting resistance in bread wheat under rainfed conditions. *Front. Agric. Sci. Eng.* **2018**, *5*, 253–261. [CrossRef]
38. Wang, X.; Liu, H.; Liu, G.; Mia, M.S.; Siddique, K.H.M.; Yan, G. Phenotypic and genotypic characterization of near-isogenic lines targeting a major 4BLQTL responsible for pre-harvest sprouting in wheat. *BMC Plant Biol.* **2019**, *19*, 348. [CrossRef]
39. Gautam, T.; Kumar, K.; Agarwal, P.; Tyagi, S.; Jaiswal, V.; Gahlaut, V. Development of white-grain pre-harvest sprouting tolerant and pyramided protein-rich leaf rust resistant wheats using molecular breeding. (Version 1). *Res. Sq.* **2021**. *preprint*. [CrossRef]
40. He, J.; Zhang, D.; Chen, X.; Li, Y.; Hu, M.; Sun, S. Identification of QTLs and a candidate gene for reducing pre-harvest sprouting in Aegilops tauschii–Triticum aestivum chromosome segment substitution lines. *Int. J. Mol. Sci.* **2021**, *22*, 3729. [CrossRef]
41. Sharma, S.K.; Dhaliwal, H.S.; Multani, D.S.; Bains, S.S. Inheritance of preharvest sprouting tolerance in *Triticum aestivum* and its transfer to an amber-grained cultivar. *J. Hered.* **1994**, *85*, 312–314. [CrossRef]
42. Singh, K.A.; Knox, R.E.; Clarke, J.M.; Clarke, F.R.; Singh, A.; DePauw, R.M.; Cuthbert, R.D. Genetics of pre-harvest sprouting resistance in a cross of Canadian adapted durum wheat genotypes. *Mol. Breed.* **2014**, *33*, 919–929. [CrossRef]
43. Huang, X.Q.; Cloutier, S.; Lycar, L.; Radovanovic, N.; Humphreys, D.G.; Noll, J.S. Molecular detection of QTLs for agronomic and quality traits in a doubled haploid population derived from two Canadian wheats (*Triticum aestivum* L.). *Theor. Appl. Genet.* **2006**, *113*, 753–766. [CrossRef]
44. Guzman, C.; Peña, R.J.; Singh, R.; Autrique, E.; Dreisigacker, S.; Crossa, J. Wheat quality improvement at CIMMYT and the use of genomic selection on it. *Appl. Transl. Genom.* **2016**, *11*, 3–8. [CrossRef]
45. Mokone, M. Understanding the Wheat Import Tariff. 2017. Available online: https://www.grainsa.co.za/understanding-the-wheat-import-tariff (accessed on 29 October 2021).
46. Nuttalla, J.G.; O'Learya, G.J.; Panozzoa, J.F.; Walkera, C.K.; Barlowb, K.M.; Fitzgerald, G.J. Models of grain quality in wheat—A review. *Field Crops Res.* **2017**, *202*, 136–145. [CrossRef]
47. Tadele, Z. Raising crop productivity in Africa through intensification: A review. *Agronomy* **2017**, *7*, 22. [CrossRef]

48. Kuzay, S.; Xu, Y.; Zhang, J.; Katz, A.; Pearce, S.; Su, Z. Identification of a candidate gene for a QTL for spikelet number per spike on wheat chromosome arm 7AL by high-resolution genetic mapping. *Theor. Appl. Genet.* **2019**, *132*, 2689–2705. [CrossRef] [PubMed]
49. Lephuthing, M.; Tolmay, V.; Baloyi, T.; Hlongoane, T.; Oliphant, T.; Tsilo, T.J. Relationship of grain micronutrient concentrations and grain yield components in a doubled haploid bread wheat (*Triticum Aestivum* L.) population. *Crop Pasture Sci.* **2021**, *73*, 116–126. [CrossRef]
50. Khumalo, T.P.; Barnard, A.; Dube, E.; Tsilo, T.J. Characterization of vegetative vigor of two doubled-haploid wheat populations. *J. Crop Improv.* **2021**, 1–19. [CrossRef]
51. ARC. *Agricultural Research Council Guidelines for the Production of Small Grains in the Winter Rainfall Area*; ARC Small Grain Institute: Bethlehem, South Africa, 1993.
52. ARC. *Agricultural Research Council Guidelines for the Production of Small Grains in the Summer Rainfall Area*; ARC Small Grain Institute: Bethlehem, South Africa, 1999.
53. VSN International. *Genstat for Windows*, 18th ed.; VSN International: Hemel, Hempstead, UK, 2015. Available online: www.genstat.co.uk (accessed on 12 June 2019).
54. Federer, W.T. Augmented designs with one-way elimination of heterogeneity. *Biometrics* **1961**, *17*, 447–473. [CrossRef]
55. Tsilo, T.J.; Kolmer, J.A.; Anderson, J.A. Molecular mapping and improvement of leaf rust resistance in wheat breeding lines. *Phytopathology* **2014**, *104*, 865–870. [CrossRef]
56. RStudio Team. *RStudio: Integrated Development for R*; RStudio, Inc.: Boston, MA, USA, 2019. Available online: http://www.rstudio.com/ (accessed on 15 January 2019).
57. van Ooijen, J.W. *JoinMap 4, Software for the Calculation of Genetic Linkage Maps in Experimental Populations*; Kyazma B.V.: Wageningen, The Netherlands, 2006.
58. Stam, P. Construction of integrated genetic linkage maps by means of a new computer package: JoinMap. *Plant J.* **1993**, *3*, 739–744. [CrossRef]
59. Kosambi, D.D. The estimation of map distances from recombination values. *Ann. Eugen.* **1943**, *12*, 172–175. [CrossRef]
60. Wang, S.; Basten, C.J.; Zeng, Z.B. *Windows QTL Cartographer 2.5*; Department of Statistics, North Carolina State University: Raleigh, NC, USA, 2012.
61. McIntosh, R.A.; Yamazaki, Y.; Devos, K.M.; Dubcovsky, J.; Rogers, W.J.; Appels, R. Catalogue of Gene Symbols for Wheat. In Tenth International Wheat Genetics Symposium, Paestum, Italy, 2003. Available online: https://wheat.pw.usda.gov/ggpages/wgc/98/intro.htm#Intro6 (accessed on 23 May 2015).
62. Alipour, H.; Bai, G.; Zhang, G.; Bihamta, M.R.; Mohammadi, V.; Peyghambari, S.A. Imputation accuracy of wheat genotyping-by-sequencing (GBS) data using barley and wheat genome references. *PLoS ONE* **2019**, *14*, e0208614. [CrossRef]
63. Liu, C.; Sukumaran, S.; Jarquin, D.; Crossa, J.; Dreisigacker, S.; Sansaloni, C.; Reynolds, M. Comparison of Array- and Sequencing-based Markers for Genome Wide Association Mapping and Genomic Prediction in Spring Wheat. *Crop Sci.* **2019**, *60*, 211–225. [CrossRef]
64. Zou, C.; Karn, A.; Reisch, B.; Nguyen, A.; Sun, Y.; Bao, Y. Haplotyping the *Vitis* collinear core genome with rhAmpSeq improves marker transferability in a diverse genus. *Nat. Commun.* **2020**, *11*, 413. [CrossRef] [PubMed]
65. Elshire, R.J.; Glaubitz, J.C.; Sun, Q.; Poland, J.A.; Kawamoto, K.; Buckler, E.S.; Mitchell, S.E. A robust, simple genotyping-by-sequencing (GBS) approach for high diversity species. *PLoS ONE* **2011**, *6*, e19379. [CrossRef] [PubMed]
66. Heslot, N.; Rutkoski, J.; Poland, J.; Jannink, J.L.; Sorrells, M.E. Impact of marker ascertainment bias on genomic selection accuracy and estimates of genetic diversity. *PLoS ONE* **2013**, *8*, e74612. [CrossRef] [PubMed]
67. Liu, Y.; Zeng, Z.-B. A general mixture model approach for mapping quantitative trait loci from diverse cross designs involving multiple inbred lines. *Genet. Res.* **2000**, *75*, 345–355. [CrossRef]
68. Qu, P.; Wang, J.; Wen, W.; Gao, F.; Liu, J.; Xia, X. Construction of consensus genetic map with applications in gene mapping of wheat (*Triticum aestivum* L.) using 90K SNP Array. *Front. Plant Sci.* **2021**, *12*, 1777. [CrossRef] [PubMed]
69. Allen, A.M.; Barker, G.L.; Wilkinson, P.; Burridge, A.; Winfield, M.; Coghill, J. Discovery and development of exome-based, co-dominant single nucleotide polymorphism markers in hexaploid wheat (*Triticum aestivum* L.). *Plant Biotechnol.* **2013**, *11*, 279–295. [CrossRef]
70. Mackay, T.F.C. The genetic architecture of quantitative traits: Lessons from Drosophila. *Curr. Opin. Genet. Dev.* **2004**, *14*, 253–257. [CrossRef] [PubMed]
71. Miles, C.M.; Wayne, M. Quantitative Trait Locus (QTL) Analysis—What Statistical Method Would You Use to Analyze Complex Traits? *Nat. Educ.* **2008**. Available online: https://www.nature.com/scitable/topicpage/quantitative-trait-locus-qtl-analysis-53904 (accessed on 11 January 2019).
72. Kulwal, P.L.; Mir, R.R.; Kumar, S.; Gupta, P.K. QTL analysis and molecular breeding for seed dormancy and pre-harvest sprouting tolerance in bread wheat. *J. Plant Biol.* **2010**, *37*, 59–74.
73. Marzougui, S.; Sugimoto, K.; Yamanouchi, U.; Shimono, M.; Hoshino, T.; Hori, K. Mapping and characterization of seed dormancy QTLs using chromosome segment substitution lines in rice. *Theor. Appl. Genet.* **2012**, *124*, 893–902. [CrossRef] [PubMed]
74. Barrero, J.M.; Cavanagh, C.; Verbyla, K.L.; Tibbits, J.F.; Verbyla, A.P.; Huang, B.E. Transcriptomic analysis of wheat near-isogenic lines identifies *PM19-A1* and *A2* as candidates for a major dormancy QTL. *Genome Biol.* **2015**, *16*, 93. [CrossRef] [PubMed]
75. Mares, D.J.; Mrva, K. Wheat grain preharvest sprouting and late maturity alpha-amylase. *Planta* **2014**, *240*, 1167–1178. [CrossRef] [PubMed]

76. Mares, D.J. Genetic studies of sprouting tolerance in red and white wheats. In *Pre- Harvest Sprouting in Cereals 1992*; Walker-Simmons, M.K., Ried, J.L., Eds.; American Association of Cereal Chemists: St. Paul, MN, USA, 1993; pp. 21–29.
77. Biddulph, T.B.; Plummer, J.A.; Setter, T.L.; Mares, D.J. Influence of high temperature and terminal moisture stress on dormancy in wheat (*Triticum aestivum* L.). *Field Crops Res.* **2007**, *103*, 139–153. [CrossRef]
78. DAFF. Production Guideline for Wheat. 2016. Available online: https://www.daff.gov.za/wheat (accessed on 20 September 2017).
79. Wang, B.; Liu, H.; Liu, Z.; Dong, X.; Guo, J.; Li, W. Identification of minor effect QTLs for plant architecture related traits using super high density genotyping and large recombinant inbred population in maize (*Zea mays*). *BMC Plant Biol.* **2018**, *18*, 17. [CrossRef] [PubMed]
80. Collard, B.C.Y.; Jahufer, M.Z.Z.; Brouwer, J.B.; Pang, E.C.K. An introduction to markers, quantitative trait loci (QTL) mapping and marker-assisted selection for crop improvement: The basic concepts. *Euphytica* **2005**, *142*, 169–196. [CrossRef]
81. Almeida, G.D.; Makumbi, D.; Magorokosho, C.; Nair, S.; Borém, A.; Ribaut, J.M. QTL mapping in three tropical maize populations reveals a set of constitutive and adaptive genomic regions for drought tolerance. *Theor. Appl. Genet.* **2012**, *126*, 583–600. [CrossRef]
82. Stange, M.; Utz, H.F.; Schrag, T.A.; Melchinger, A.E.; Würschum, T. High-density genotyping: An overkill for QTL mapping? Lessons learned from a case study in maize and simulations. *Theor. Appl. Genet.* **2013**, *126*, 2563–2574. [CrossRef]
83. Lin, M.; Zhang, D.; Liu, S.; Zhang, G.; Yu, J.; Fritz, A.K.; Bai, G. Genome-wide association analysis on pre-harvest sprouting resistance and grain color in U.S. winter wheat. *BMC Genom.* **2016**, *17*, 794. [CrossRef]
84. Singh, R.; Matus-Cádiz, M.; Båga, M.; Hucl, P.; Chibbar, R.N. Genetic Mapping of Pre-Harvest Sprouting Resistance Loci in Bread Wheat (*Triticum aestivum* L.). 2006. Available online: https://harvest.usask.ca/bitstream/handle/10388/9460/R.%20Singh%20et%20al.%2C%202006.pdf?sequence=1&isAllowed=y (accessed on 15 June 2021).
85. Fofana, B.; Humphreys, G.; Rasul, G.; Cloutier, S.; Somers, D. Assessment of molecular diversity at QTLs for preharvest sprouting resistance in wheat using microsatellite markers. *Genome* **2008**, *51*, 375–386. [CrossRef]
86. Zhou, S.H.; Lin, F.U.; Wu, Q.H.; Chen, J.J.; Chen, Y.X.; Xie, J.Z. QTL mapping revealed *TaVp-1A* conferred pre-harvest sprouting resistance in wheat population Yanda 1817×Beinong 6. *J. Integr. Agric.* **2017**, *16*, 435–444. [CrossRef]
87. Mori, M.; Uchino, N.; Chono, M.; Kato, K.; Miura, H. Mapping QTLs for grain dormancy on wheat chromosome 3A and the group 4 chromosomes, and their combined effect. *Theor. Appl. Genet.* **2005**, *110*, 1315–1323. [CrossRef] [PubMed]
88. Munkvold, J.D.; Tanaka, J.; Benscher, D.; Sorrells, M.E. Mapping quantitative trait loci for preharvest sprouting resistance in white wheat. *Theor. Appl. Genet.* **2009**, *119*, 1223–1235. [CrossRef]
89. Somyong, S.; Ishikawa, G.; Munkvold, J.D.; Tanaka, J.; Benscher, D.; Cho, Y.G.; Sorrells, M.E. Fine mapping of a preharvest sprouting QTL interval on chromosome 2B in white wheat. *Theor. Appl. Genet.* **2014**, *127*, 1843–1855. [CrossRef] [PubMed]
90. Zhou, Y.; Tang, H.; Cheng, M.P.; Dankwa, K.O.; Chen, Z.X.; Li, Z.Y. Genome-wide association study for pre-harvest sprouting resistance in a large germplasm collection of Chinese wheat landraces. *Front. Plant Sci.* **2017**, *8*, 401. [CrossRef] [PubMed]
91. Nakamura, S.; Abe, F.; Kawahigashi, H.; Nakazono, K.; Tagiri, A.; Matsumoto, T. A wheat homolog of *MOTHER OF FT* AND *TFL1* acts in the regulation of germination. *Plant Cell* **2011**, *23*, 3215–3229. [CrossRef]
92. Rutter, M.; Moffitt, T.E.; Caspi, A. Gene-environment interplay and psychopathology: Multiple varieties but real effects. *J. Child Psychol. Psychiatry* **2006**, *47*, 226–261. [CrossRef]
93. Hospital, F. Challenges for effective marker-assisted selection in plants. *Genetica* **2009**, *136*, 303–310. [CrossRef]
94. Ogbonnaya, F.C.; Rasheed, A.; Okechukwu, E.C.; Jighly, A.; Makdis, F.; Wuletaw, T. Genome-wide association study for agronomic and physiological traits in spring wheat evaluated in a range of heat prone environments. *Theor. Appl. Genet.* **2017**, *130*, 1819–1835. [CrossRef]
95. Jannink, J.-L.; Bink, M.C.A.M.; Jansen, R.C. Using complex plant pedigrees to map valuable genes. *Trends Plant Sci.* **2001**, *6*, 337–342. [CrossRef]
96. Shen, L.; Courtois, B.; McNally, K.L.; Robin, S.; Li, Z. Evaluation of near-isogenic lines of rice introgressed with QTLs for root depth through marker-aided selection. *Theor. Appl. Genet.* **2001**, *103*, 75–83. [CrossRef]